Journal of Power Sources 248 (2014) 831–838

Contents lists available at ScienceDirect

Journal of Power Sources

journal homepage: www.elsevier.com/locate/jpowsour

Plasma graft-polymerization for synthesis of highly stable hydroxide exchange membrane

Jue Hu [a], Chengxu Zhang [a,*], Lin Jiang [b], Shidong Fang [a], Xiaodong Zhang [a], Xiangke Wang [a], Yuedong Meng [a]

[a] Institute of Plasma Physics, Chinese Academy of Sciences, P.O. Box 1126, 230031, PR China
[b] Faculty of Science, Kunming University of Science and Technology, 650500, PR China

HIGHLIGHTS

- Successfully introduced functional groups into PEK-C matrix via plasma graft-polymerization.
- Plasma graft-polymerization enables high preservation in polymer backbone and functional groups.
- The obtained membranes possess high chemical stability.

GRAPHICAL ABSTRACT

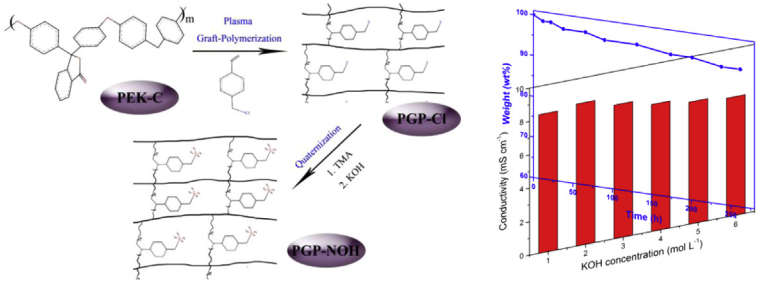

ARTICLE INFO

Article history:
Received 20 July 2013
Received in revised form
22 September 2013
Accepted 23 September 2013
Available online 12 October 2013

Keywords:
Plasma graft-polymerization
Hydroxide exchange membrane
Chemical stability
Benzyltrimethylammonium group
Cardo polyetherketone powder

ABSTRACT

A novel plasma graft-polymerization approach is adopted to prepare hydroxide exchange membranes (HEMs) using cardo polyetherketone powders (PEK-C) and vinylbenzyl chloride. The benzylic chloromethyl groups can be successfully introduced into the PEK-C polymer matrix via plasma graft-polymerization. This approach enables a well preservation in the structure of functional groups and formation of a highly cross-linked structure in the membrane, leading to an improvement on the stability and performance of HEMs. The chemical stabilities, including alkaline and oxidative stability, are evaluated under severe conditions by measuring hydroxide conductivity and weight changes during aging. The obtained PGP-NOH membrane retains 86% of the initial hydroxide conductivity in 6 mol L^{-1} KOH solution at 60 °C for 120 h, and 94% of the initial weight in 3 wt% H_2O_2 solution at 60 °C for 262 h. The PGP-NOH membrane also possesses excellent thermal stability (safely used below 120 °C), alcohol resistance (ethanol permeability of 6.6×10^{-11} m^2 s^{-1} and diffusion coefficient of 3.7×10^{-13} m^2 s^{-1}), and an acceptable hydroxide conductivity (8.3 mS cm^{-1} at 20 °C in deionized water), suggesting a good candidate of PGP-NOH membrane for HEMFC applications.

1. Introduction

Fuel cells (FCs), which are expected to provide clean and efficient energy sources for stationary, automobile and portable electronic device applications, have attracted considerable attention as means of securing a sustainable future for mankind [1]. Among the several different types of FCs, polymer electrolyte fuel cell (PEFC) as a potential future power source for zero-emission vehicles has been the most developed one in the past two decades due to its rapid startup and high power density [2,3]. Since the development of perfluorinated cation exchange membranes, such as Nafion®, PEMFCs are considered to be one of the most

* Corresponding author. Tel.: +86 551 65591378; fax: +86 551 65591310.
E-mail address: chxzhang@ipp.ac.cn (C. Zhang).

0378-7753/$ – see front matter © 2013 Elsevier B.V. All rights reserved.
http://dx.doi.org/10.1016/j.jpowsour.2013.09.099

important technologies in the 21st century [4]. To date, significant efforts have been devoted to the development of proton exchange membrane fuel cells (PEMFCs). However, to become commercially viable, PEMFCs have to overcome a number of scientific and technological barriers: high cost by exclusive used of platinum-based catalysts and membranes, serious fuel crossover, serious corrosion and low durability in acidic environment [3,5]. Hydroxide exchange membrane fuel cell (HEMFC) is another type of PEFC that uses hydroxide exchange membrane (HEM) as the polymer electrolyte, in which hydroxide ions instead of protons are transported through the membrane. Compared with its acid analogue, several merits for HEMFC have been suggested: (i) potential for use of non-precious metal catalysts due to the structure insensitive for electro-oxidation of fuels in alkaline environment; (ii) lower fuel permeability due to the opposite direction of electro-osmotic drag; (iii) lower overpotential associated with many electrochemical reactions in alkaline condition; (iv) less serious corrosion and potentially simplified water management [6–9].

In HEMFC, the HEM is a critical component which can seriously affect the performance of the whole system. Unluckily, there is no equivalent commercially available HEM for HEMFC to Nafion® in PEMFC. Since the membrane features are far from HEMFC requirements, the researches of development on HEMs performance become crucial. Significant efforts have been focused on a noteworthy HEM system by performing a chloromethylation reaction on the polymer backbone to form benzylic chloromethyl groups, followed by quaternization and alkalization [6,10,11]. However, in the chloromethylation reaction, the chloromethyl groups are not always located into the expected position on the polymer backbone, which leads to serious side reactions and inaccurate ion-exchange capacity (IEC) values for membrane [12]. Furthermore, the chloromethylation reaction has other shortcomings, including its sluggishness and the requirement of large quantities of carcinogens, such as chloromethyl ether and bichloromethyl ether [11,13]. Another important development came from Varcoe and co-workers who prepared HEMs by radiation-grafting vinylbenzyl chloride (VBC) onto polymer matrix, such as poly(ethylene-*co*-tetrafluoroethylene) (ETFE), poly(vinylidene fluoride) (PVDF), poly(tetrafluoroethene-*co*-hexafluoropropylene) (FEP), and so on, which has been proved to be an effective way to avoid chloromethylation reaction [14–17]. However, due to the high energy level of the radiation, irradiation damage occurred in the polymer matrix to a certain extent, which could seriously affect the membrane's structure, and more importantly, the stability [14]. It is well known that in most HEMFC systems to date, alkaline was still added to the fuel, leading to an extremely severe circumstance for HEM operation. Since the HEM works in such strong alkaline and oxidative environment, new method for synthesizing HEM with excellent stability is promising [18].

More recently, we have developed a novel plasma grafting approach to prepare HEM, which is demonstrated to be a mild and efficient method for introducing benzylic chloromethyl groups onto the polymer backbone and preserving the polymer structure [19]. To further improve the stability of the membrane, a cross-linked structure is needed [4]. Herein, plasma graft-polymerization was adopted to synthesize HEMs. In the plasma graft-polymerization process, exciting species within plasma bombard with the polymer matrix to create active sites for binding of functional groups, and in the same time, attack with monomer to prepare active species for polymerizing of high cross-linked structure on the polymer matrix [20]. By employing the plasma graft-polymerization approach, benzylic chloromethyl groups can be efficient introduced into the polymer backbone. In addition, this approach enables a well preservation in the structure of the polymer backbone and functional groups, leading to an improvement on the stability and performance of HEMs [21]. Furthermore, since the plasma bombardment, grafting and polymerization processes simultaneously occur in gaseous phase, HEM synthesis can be simplified and the problem of liquid waste pollution is expected to be resolved.

The object of the present study is to prepare HEM by the plasma graft-polymerization approach using cardo polyetherketone (PEK-C) powders as the substrate polymer matrix and VBC as the monomer. The chemical structure, physicochemical and electrochemical characteristics of the obtained membranes, including ionic exchange capacity, water uptake, swelling degree, thermal stability, alkaline stability, oxidative stability, ionic conductivity and ethanol permeability, were evaluated.

2. Experimental

2.1. Materials

Cardo polyetherketone (PEK-C) powder (particle size around 50 μm) was obtained from Xuzhou Engineering Plastic Factory (China). Vinylbenzyl chloride (VBC, 95 wt%) was received from Alfa Aesar®. Trimethylamine (TMA, 33 wt%), potassium hydroxide (KOH, AR grade), ethanol (EtOH, AR grade), hydrochloric acid (HCl, 37 wt %) and dimethylformamide (DMF, AR grade) were purchased from Shanghai Chemical Reagent Store (China). High purity hydrogen (H_2, 99.999%), and argon (Ar, 99.999%) were obtained from Shangyuan Gas Co. Ltd. (China). Deionized water was used in the experiments. All reagents were used as received without further purification.

2.2. Synthesis of plasma graft-polymerized hydroxide exchange membranes

There are two steps in preparation of plasma graft-polymerized HEMs, as shown in Scheme 1: (i) plasma graft-polymerization of VBC monomer into PEK-C polymer matrix; (ii) quaternization of benzylic chloromethyl groups into benzyltrimethylammonium cationic groups ($-N^+(CH_3)_3OH^-$).

The plasma graft-polymerization process was carried out in an inductively coupled plasma (ICP) system, depicted in Fig. 1. The device consists of a cylindrical Pyrex glass tube, a radio frequency (RF) power supply, a monomer heater with temperature controller, gas mass flow controllers and a mechanical booster pump. The ICP sustained by a RF power supply inside the brass coil. There are two pieces of Nylon screens in the middle of the Pyrex glass tube with a gap of 100 mm where PEK-C powders located in. Before plasma polymerization of VBC monomer, PEK-C powders were treated by argon plasma under the discharge power of 150 W for 10 min. VBC monomer carried by hydrogen was inlet into the reactor through the gas lines, which were wrapped by heating wires to prevent the polymerization and condensation of VBC on the inner walls of gas lines. The experimental details of plasma graft-polymerization process were: 20 W for the discharge power, 20 Pa for the partial pressure of argon, 60 Pa for the reactor total pressure and 2 h for the reaction time.

The obtained PEK-*gp*-PVBC (PGP-Cl) powders (2 g) were dissolved in DMF to form a 10 wt% solution. A part of the solution was cast onto a flat, clean glass plate and dried in vacuum oven at 50 °C for 12 h and then further dried in vacuum oven at 80 °C for 12 h, after which the film (PGP-Cl) was removed from the glass plate by immersing it in deionized water. In the quaternization process, the rest part of the solution (PGP-Cl) was bubbled with TMA gas at a flow rate of 100 mL min^{-1} for 0.5 h. The resulting quaternized PGP-Cl (PGP-NCl) solution was cast into film using the same condition of preparing PGP-Cl membrane. In order to replace the Cl^- anion in

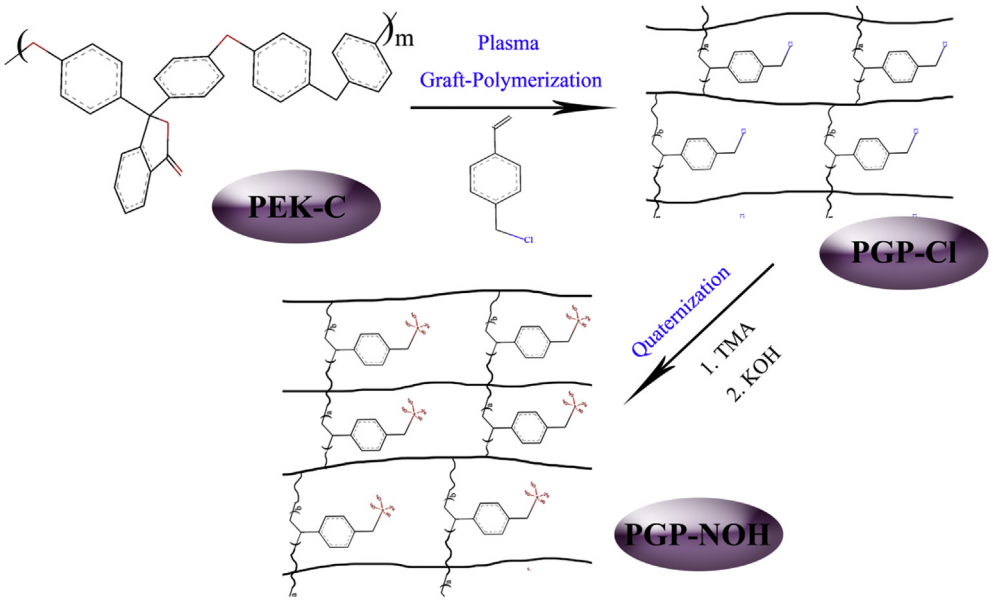

Scheme 1. Synthesis of high cross-linked hydroxide exchange membrane by plasma graft-polymerization.

the polymer with OH^-, the PGP-NCl membrane was immersed in 1 mol L^{-1} KOH solution at room temperature for 48 h. Finally, the obtained membrane (PGP-NOH) was washed by deionized water to remove any trapped KOH and finally immersed in deionized water for more than 48 h with frequent water changes.

2.3. Chemical characterization of membranes

The chemical structure of the obtained membranes were analyzed by Fourier transform infrared spectroscopy (FT-IR), X-ray photoelectron spectroscopy (XPS) and thermogravimetric analysis (TGA). The FT-IR analysis was performed in the range of 4000–670 cm^{-1} using a Nicolet NEXUS 870 spectrometer. The spectra were obtained with subtracting the contributions from H_2O (gas) and CO_2 after 64 scans at 2 cm^{-1} resolution. The XPS analysis was carried out with a Thermo ESCALAB 250 spectroscopy at a power of 150 W. The information of spectrometer detail and measurement condition can be found in our previous literature [22]. The spectra were calibrated with respect to the C 1s peak at 284.6 eV. The curves were fitted with symmetrical Lorentz–Gauss functions. The TGA measurement was used to observe the chemical structure and thermal stability of the obtained membranes by using DTG-60H (SHIMADZU, Japan) thermal analyzer in flowing nitrogen at a scanning rate of 10 °C min^{-1} from ambient temperature to 800 °C.

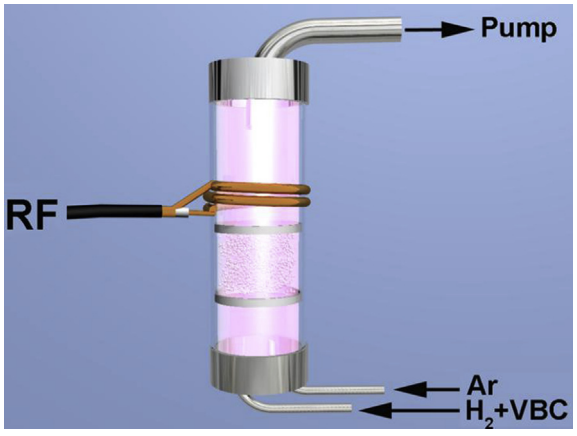

Fig. 1. Schematic diagram of the apparatus for plasma graft-polymerization.

2.4. Ion-exchange capacity of membranes

In order to evaluate the capability of hydroxide ion transport, the ion-exchange capacity (IEC) of PGP-Cl and PGP-NOH membranes was measured by classical back titration method [21]. For IEC measurement, dry membranes were accurately weighed and then converted to the OH^- form by immersing in 1 mol L^{-1} KOH solution for 48 h. Three pieces of samples from the same membrane were respectively equilibrated with 25 ml 0.05 mol L^{-1} HCl solution for 48 h. After that the HCl solution was back titrated by 0.05 mol L^{-1} NaOH solution. IEC values of the samples can be calculated according to Eq. (1):

$$\mathrm{IEC} = \frac{n_{1,\mathrm{HCl}} - n_{2,\mathrm{HCl}}}{m_{\mathrm{dry}}} \quad (1)$$

where m_{dry} is the mass (g) of the dried sample, $n_{1,HCl}$ and $n_{2,HCl}$ are the amount (mmol) of HCl required before and after equilibrium, respectively. The IEC value of the testing membrane is the average value of the three samples calculated from Eq. (1).

2.5. Ethanol uptake and swelling degree of membranes

The water uptake (WU) and swelling degree (SD) were carried out by measuring the change of weight and thickness between the membrane before and after immersion in deionized water, respectively. The weight and thickness of the wet membrane were measured after wiping excess surface solution. The wet membrane was then dried in vacuum oven at 60 °C until a constant weight was obtained. The weight and thickness of the dry membrane were measured. The WU and SD of the testing membranes could be calculated using Eqs. (2) and (3), respectively.

$$\mathrm{WU}\% = \frac{m_{\mathrm{wet}} - m_{\mathrm{dry}}}{m_{\mathrm{dry}}} \times 100\% \quad (2)$$

$$SD\% = \frac{T_{wet} - T_{dry}}{T_{dry}} \times 100\% \quad (3)$$

where m_{wet} is the mass (g) of a wet membrane and m_{dry} is one of a dry membrane. T_{wet} is the thickness (μm) of a wet membrane and T_{dry} is one of a dry membrane, measured by micrometer (Mitutoyo, Japan). The WU and SD values of the testing membrane is the average value of the three samples.

2.6. Ionic conductivity and ethanol permeability of PGP-NOH membrane

Ionic conductivity and alcohol permeability are crucial criteria for evaluating the membrane performance. As described in our previous literature, the hydroxyl ion conductivity was carried out by three-electrode AC impedance spectroscopy using an Autolab potentiostat/galvanostat (IM6e, Zahner, Germany) in deionized water at 20 °C [20]. Before testing the PGP-NOH membrane samples (3.0 cm × 4.0 cm) were hydrated in deionized water until neutral pH was obtained. The hydrated membrane was then rapidly placed between two polytetrafluoroethylene (PTFE) plates after removing the surface water. The testing cell was placed in a chamber which filled with deionized water to keep the water content of membrane samples constant during the measurements. The hydroxyl ion conductivity (σ_{OH^-}) could be calculated using the relation:

$$\sigma_{OH^-} = \frac{l}{R_m A} \quad (4)$$

where R_m is the membrane resistance (Ω) obtained from the AC impedance data which derived from the intersect of the high frequency semicircle on a complex impedance plane with the Z' axis. l is the distance (cm) between the working electrode and reference electrode (2 cm). A is the cross-sectional area (cm^2) of the membrane.

The open circuit potential method to establish the calibration curve of potential shift against ethanol concentration and measure the ethanol permeability of PGP-NOH membrane was described in Refs. [21,23,24]. The membrane sample was clamped between two compartments of a diffusion cell connected with an O-ring seal. The membrane cross-sectional area exposed to the solution was 2.0 cm^2. One compartment (A) was loaded with 1 mol L^{-1} KOH and 1 mol L^{-1} EtOH solution. Another one (B) was filled with an equal volume of 1 mol L^{-1} KOH solution. A Pt foil was used as counter electrode and a saturated calomel electrode (SCE) was used as reference electrode. Gas diffusion electrode (GDE) prepared by plasma technology with platinum loading of 0.05 mg cm^{-2} was used as working electrode by flowing pure oxygen [25]. In the absence of ethanol, the potential of GDE in 1 mol L^{-1} KOH solution represents the standard electrode potential (E^{θ}). Due to the oxidation of ethanol in the Pt catalyst surface, the potential of GDE drops if adding the ethanol into KOH solution. The ethanol concentration (c_{EtOH}) could be estimated by the GDE potential drop (ΔE) from the Eq. (5):

$$\Delta E = -a \ln c_{EtOH} \quad (5)$$

The ethanol permeability (P) of the membrane can be estimated from the relationship between the concentration of ethanol in KOH solution only compartment ($c_{EtOH,B}$) and the permeation time (t), as shown in Eq. (6).

$$\frac{V_B L_m}{c_{EtOH,A} S} c_{EtOH,B}(t) = P\left(t + \frac{L_m^2}{6D}\right) \quad (6)$$

where L_m and S are the membrane thickness (m) and membrane active area (m^2) of measured membrane, respectively. V_B and $c_{EtOH,A}$ are the volume of solution in compartment B (m^3) and concentration of ethanol in compartment A (1 mol L^{-1}), respectively. Ethanol diffusion coefficient (D) can also be investigated through Eq. (6).

2.7. Chemical stability of PGP-NOH membrane

The alkaline stability of the PGP-NOH membrane was investigated by soaking the membrane samples in KOH solution at 60 °C for 120 h, and measured for hydroxyl ion conductivity in deionized water at 20 °C after the free KOH was completely removed. The KOH solution was renewed for every 12 h. For oxidative stability, the testing membrane samples were immersed the samples into 3 wt% H_2O_2 solution at 60 °C for more than 240 h. The H_2O_2 solution was renewed for every 12 h and the weight loss of the sample was measured at certain time intervals.

3. Results and discussion

3.1. Chemical structure characterization

FT-IR spectra of PEK-C, PGP-Cl and PGP-NOH samples were shown in Fig. 2. From Fig. 2, the FT-IR spectra of all the membranes were similar. All the spectra showed four bands at 1659 cm^{-1}, 1770 cm^{-1}, 1240 cm^{-1} and 1500 cm^{-1}, which related to the stretching vibrations of carbonyls in ketone group (–Ar–C(=O)–Ar–) and phenolphthalein group, the C=C stretch of the ether group (–Ar–O–Ar–) and benzene, respectively, suggesting that the structure of the PEK-C matrix was not destroyed by the plasma bombardment and graft-polymerization [26,27]. The FT-IR spectrum of PGP-Cl membrane showed absorptions at 704 cm^{-1}, 780 cm^{-1} and 844 cm^{-1}, not present for PEK-C, corresponding to stretching vibration of C–Cl bond, confirming the successful grafting of VBC into the PEK-C backbone [28–30]. The bands at 795 cm^{-1}, 3400 cm^{-1} and 3450 cm^{-1} of PGP-NOH membrane, not present for PGP-Cl, were assigned to rocking mode of CH_2, N–H stretching and O–H stretching, respectively, indicating the successful quaternization and alkalization of benzylic chloromethyl groups into $-N^+(CH_3)_3OH^-$ groups [31–33].

To acquire more information on the chemical structure characteristics of the resulting membranes, XPS data of PGP-Cl and PGP-

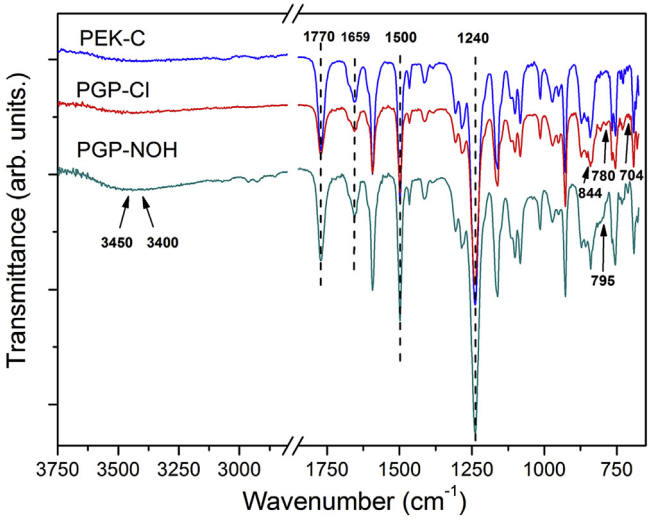

Fig. 2. FT-IR spectra of PEK-C, PGP-Cl and PGP-NOH membranes.

NOH membranes were analyzed. The concentration of Cl in the PGP-Cl membrane was 0.92 at% according to the XPS data. Fig. 3a showed the Cl 2p core-level XPS spectrum of the PGP-Cl membrane, which could be curve-fitted with two spin-orbit-split doublets: doublet at 199.9 ± 0.2 eV and 201.6 ± 0.2 eV related to the covalently bonded chlorine species (C—Cl) in benzylic chloromethyl groups, and another doublet at 197.4 ± 0.2 eV and 199.0 ± 0.2 eV attributable to the ionic chloride (Cl^-) [34,35]. The quantitative analysis confirms the successful grafting and high preservation of benzylic chloromethyl in PGP-Cl membrane in the plasma graft-polymerization process. As shown in Fig. 3b, the C 1s peak can be curve-fitted with four peaks [35–38]: peak (1) at 284.3 ± 0.2 eV assigned as the sp^2 carbon atoms (C═C); peak (2) at 284.8 ± 0.2 eV attributed to the sp^3 carbon atoms (C—C and C—H); peak (3) at 286.1 ± 0.2 eV corresponded to sp^3 carbon bonded to one nitrogen atom (C—N), chlorine atom (C—Cl) and oxygen atom (C—O); peak (4) at 287.2 ± 0.2 eV related to the carbonyl groups (C═O). The increase in the C—N, C—O and C—Cl fraction of PGP-NOH membrane indicates the successful quaternization and alkalization of PGP-Cl membrane. Fig. 3c shows the N 1s core-level XPS spectra of the PGP-Cl and PGP-NOH membranes. The peak at 401.7 eV for PGP-NOH membrane, not present for PGP-Cl, was assigned to the positively charged nitrogen (N^+) [39–41]. This may further confirm that the functional $-N^+(CH_3)_3OH^-$ groups have been introduced into the PEK-C matrix via plasma graft-polymerization and quaternization.

According to the TGA trace, shown in Fig. 4, PEK-C polymer decomposed mainly at 400 °C due to the splitting off of the phenolphthalein groups [11]. There are two major weight loss stages for the PGP-Cl membrane: stage (1) in the range of 73–270 °C related to the degradation of trapped VBC monomer [14]; and stage (2) mainly at 430 °C attributed to the splitting off of the phenolphthalein groups. The degradation temperature of phenolphthalein groups in PGP-Cl membrane is higher than that in PEK-C polymer, indicating a positive effect of plasma graft-polymerization on improving a highly cross-linked structure of membrane. For PGP-NOH membrane, two stages of weight loss behavior are observed. The first degradation in the range of 120–290 °C is corresponding to the loss of the benzyltrimethylammonium groups. The second weight loss region of

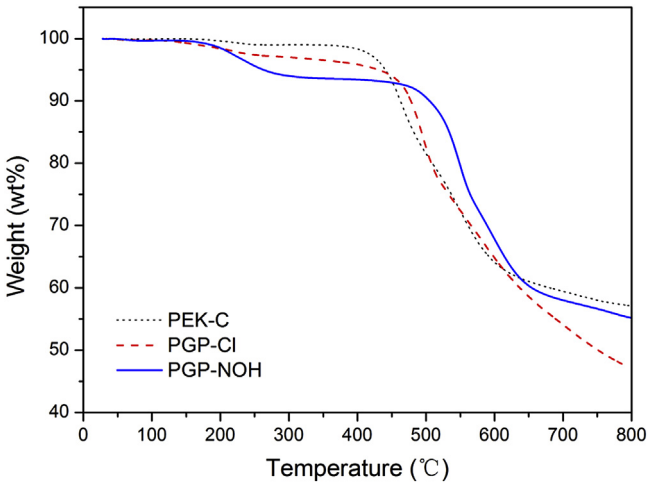

Fig. 4. Thermogravimetric analysis of PEK-C, PGP-Cl and PGP-NOH membranes.

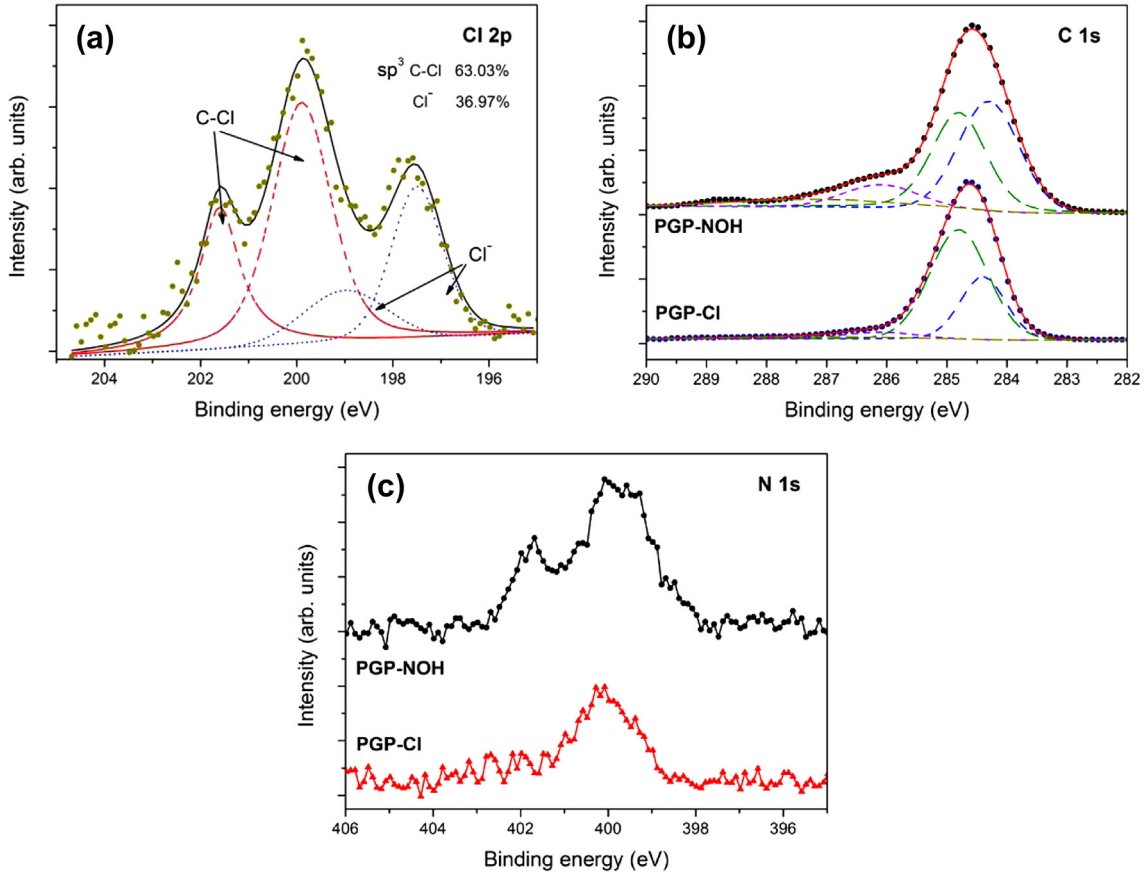

Fig. 3. XPS spectra of (a) Cl 2p for PGP-NOH membrane, (b) C 1s and (c) N 1s for PGP-Cl and PGP-NOH membranes.

PGP-NOH membrane at temperature above 480 °C ascribed to the degradation of the phenolphthalein groups in the side chain and the membrane backbone.

3.2. IEC, ethanol uptake and swelling degree

The thickness, IEC, WU and SD values of the PGP-Cl and PGP-NOH membranes were shown in Table 1. The IEC value of PGP-NOH membrane is 0.67 mmol g^{-1}, which is higher than that of PGP-Cl membrane (0.08 mmol g^{-1}), indicating the introduction of functional $-N^{+}(CH_3)_3OH^{-}$ groups in the PGP-NOH membrane.

Compared to the IEC value in the literature (0.11 mmol g^{-1}), the capability of hydroxide transport of our membrane can be accepted [11]. The PGP-Cl and PGP-NOH membranes exhibit excellent solvent resistance according to the WU and SD values. The PGP-NOH membrane exhibit a good dimensional stability with the SD value only 12.96% at the room temperature. Both the WU and SD values of PGP-NOH membrane are higher than that of PGP-Cl membrane due to the improvement of hydrophilic nature by introducing hydroxide-exchange groups into the membrane.

3.3. Ionic conductivity and ethanol permeability

Ionic conductivity is one of the most important property of HEMs employed in HEMFC applications. The hydroxide conductivity was calculated by Eq. (4) from the AC impedance spectroscopy and the thickness of hybrid membrane in Table 1. For comparison, the hydroxide conductivity of the commercial AHA-OH membrane (NEOSEPTA® AHA membrane OH^{-} form) was also measured under the same conditions [22]. The hydroxide conductivity of PGP-NOH membrane is 8.3 mS cm^{-1} at 20 °C, which is more than 2 times that of the AHA-OH membrane (3.5 mS cm^{-1}) [22]. To investigate the temperature dependence of the ionic conductivities of ion-exchange membrane, the relationship between $\ln \sigma_{OH^-}$ and $1000/T$ was shown in Fig. 5. The hydroxide conductivity of PGP-NOH membrane increases with increasing temperature, assuming that the conductivity followed the Arrhenius law [42]. Hydroxide transport activation energy (E_{a,OH^-}) of the PGP-NOH membrane can be obtained according to the Arrhenius equation:

$$E_{a,OH^-} = RT^2 \frac{d\ln \sigma_{OH^-}}{dT} \quad (7)$$

where T is the absolute temperature (K) and R is the pure gas constant (8.314 J mol^{-1} K^{-1}). The activation energy value of alkalinized PGP-NOH membrane is 13.59 kJ mol^{-1} (0.14 eV), which is lower than that of the commercial AHA-OH membrane in the literature (17.56 kJ mol^{-1}), indicating a lower energy barrier for carrier transfer from one free site to another in our membrane [22].

Alkaline direct alcohol fuel cells (ADAFCs) are the most common HEMFCs due to easy storage and transportation of fuels. Alcohol permeability, as a determinant of hydroxide exchange membrane for potential use in fuel cells, can seriously affect the fuel cell power density, energy conversion efficiency and fuel utilization. The relationship between potential drop (ΔE) and ethanol concentration (c_{EtOH}), and the calibration curve of ΔE against c_{EtOH} were shown in Fig. 6a. Therefore, the ethanol concentration in compartment B ($c_{EtOH,B}$) during permeation experiment can be inferred from the drop of GDE potential using Eq. (5). The relationship between $c_{EtOH,B}$ and permeation time (t) was shown in Fig. 6b. It is evident that $(V_B L_m / c_{EtOH,A} S) c_{EtOH,B}(t)$ has a linear correlation with t. According to Eq. (6), the slope and intercept of the fitting line are ethanol permeability (P) and $P(L_m^2/6D)$, respectively. The plasma graft-polymerized PGP-NOH membrane exhibits remarkable ethanol permeability of 6.6 × 10^{-11} m^2 s^{-1} at 20 °C when the concentration of ethanol in compartment A is 1 mol L^{-1}. Moreover, since the hydroxide transport through the membrane occurs in the opposite direction to the alcohol crossover in the ADAFC, the electro-osmotic drag effect may reduce the ethanol permeability and vice versa. So a low ethanol permeability of HEM may lead to an increase of hydroxide transport in the ADAFC. The diffusion coefficient (D) of PGP-NOH membrane is only 3.7 × 10^{-13} m^2 s^{-1}, based on Eq. (6) and data in Fig. 6b. The low ethanol permeability and diffusion coefficient value suggested a good performance of PGP-NOH membrane for application in ADAFCs.

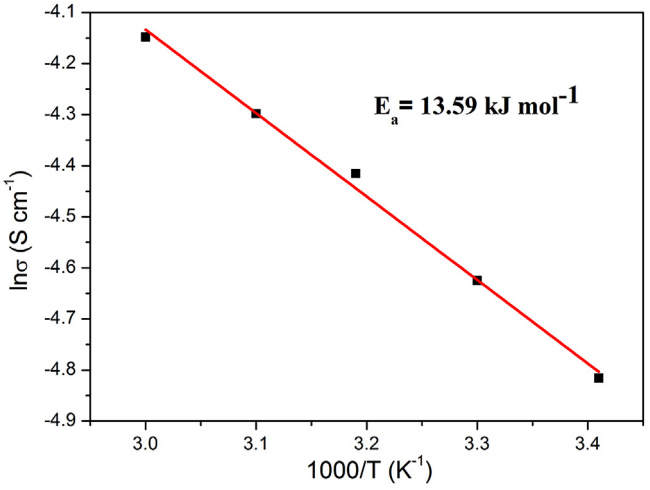

Fig. 5. Arrhenius plot showing the temperature dependence of hydroxide conductivity for PGP-NOH membrane.

Table 1
Thickness, IEC, WU and SD of the PGP-Cl and PGP-NOH membranes.

Membrane	Thickness (μm)	IEC (mmol g^{-1})	Water uptake (wt%)	Swelling degree (%)
PGP-Cl	57	0.08	5.33	3.64
PGP-NOH	60	0.67	18.13	12.96

3.4. Chemical stability and thermal stability

To investigate the alkaline stability of the obtained PGP-NOH membrane, the effects of the alkaline concentration on the hydroxide conductivity of the membrane were measured, as shown in Fig. 7. The measured conductivity ranged from 7.1 to 8.5 mS cm^{-1} after conditioning in 1–6 mol L^{-1} KOH solutions for 120 h. With increasing the concentration of KOH solution, the conductivity of the PGP-NOH membrane increases first reaching a maximum value (8.5 mS cm^{-1} for 2 mol L^{-1} KOH). This might because that more OH^{-} ions enter into the ion transport channels of PGP-NOH membrane by the force of concentration penetration. However, the ionic conductivity of the PGP-NOH membrane slightly decreased when the concentration of KOH solution increased above 2 mol L^{-1}. This might be contributed to the displacement of the $-N^{+}(CH_3)_3OH^{-}$ groups by OH^{-} via the nucleophilic substitution reaction (S_N2 pathway) [43]. At the rigid basic environment of 6 mol L^{-1} KOH solutions at 60 °C for 120 h, the residual hydroxide conductivity of the PGP-NOH membrane is still up to 86% of the initial value. The results indicate an excellent alkaline stability of the PGP-NOH membrane in a broad basic working window at

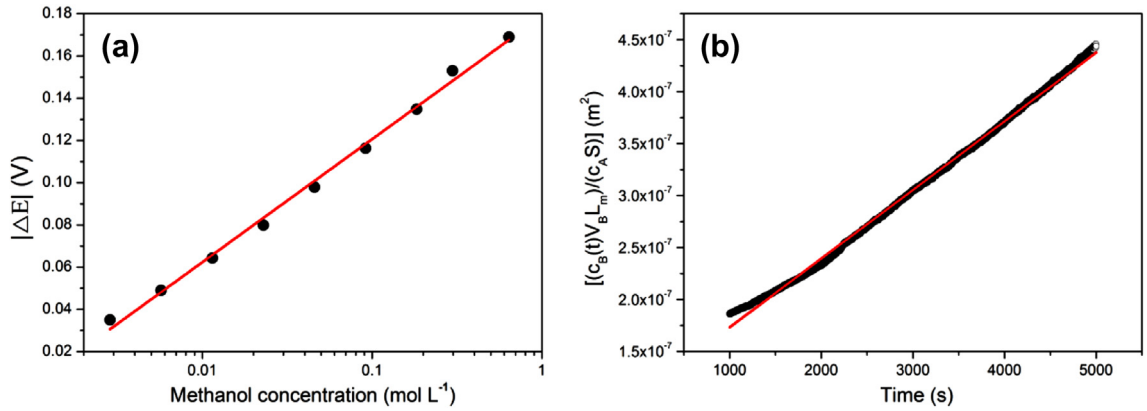

Fig. 6. (a) Potential shift against ethanol concentration. The dots are the experimental data and the line is the linear fitting of the experimental results using Eq. (5). (b) Permeability data for the PGP-NOH membrane in the ethanol concentration in compartment A of 1 mol L^{-1} at 20 °C.

temperature up to 60 °C, suggesting a good candidate of PGP-NOH membrane for HEMFC applications.

Since the hydroxide exchange membrane works in oxidative circumstances, its oxidative stability can be evaluated by durability time in strong oxidative conditions, such as H_2O_2 [11,44]. The lose in the weight of the PGP-NOH membrane over time was shown in Fig. 8. In the first 90 h, the weight loss of PGP-NOH membrane was 3.75 wt% due to the trapped free radicals within the polymer matrix by plasma bombardment [45]. In the next 172 h, the weight loss of PGP-NOH membrane was only 2.50 wt%, suggesting that the polymer backbone was not destroyed by the plasma treatment. In the whole 262 h, the residual weight of PGP-NOH membrane is still up to 94% of the initial value, indicating that the PGP-NOH membrane is quite stable in a strong oxidative condition at temperature up to 60 °C [46].

HEMs with high thermal stability are desirable since operation of HEMFCs at elevated temperature would not only reduce thermodynamic voltage losses but also improve the electro-kinetics [7]. According to the TGA and its differential curve (DrTGA), as shown in Fig. 9, the degradation in the range of 120–290 °C is corresponding to the loss of the benzyltrimethylammonium groups, indicating a great stability of the resulting PGP-NOH membrane below 120 °C [44]. The weight loss below 100 °C is corresponding to the removal of residual water trapped in the polymer matrix.

4. Conclusions

In this study, the plasma graft-polymerization approach was adopted for the first time to prepare HEMs using PEK-C powders as the substrate polymer matrix and VBC as the monomer. This approach enables the formation of high cross-linked structure on the surface of the polymer matrix, and a well preservation in the structure of the polymer backbone and functional groups, leading to an improvement on the stability of HEMs. The FT-IR, TGA and XPS analysis demonstrate that the benzylic chloromethyl groups have been successfully introduced into the PEK-C polymer matrix via plasma graft-polymerization and quaternized into benzyltrimethylammonium cationic groups. The PGP-NOH membrane possessed excellent thermal stability (safely used below 120 °C), alkaline stability, oxidative stability, alcohol resistance (ethanol permeability of 6.6×10^{-11} m^2 s^{-1} and diffusion coefficient of 3.7×10^{-13} m^2 s^{-1}), and an acceptable hydroxide conductivity (8.3 mS cm^{-1} at 20 °C in deionized water), suggesting a good candidate of PGP-NOH membrane for HEMFC applications. Further researches on the performance improvement of PGP-NOH membranes are under investigation by increasing the concentration of the monomer which is crucial in increasing the benzyltrimethylammonium group attachment onto the polymer matrix to achieve a higher ionic conductivity.

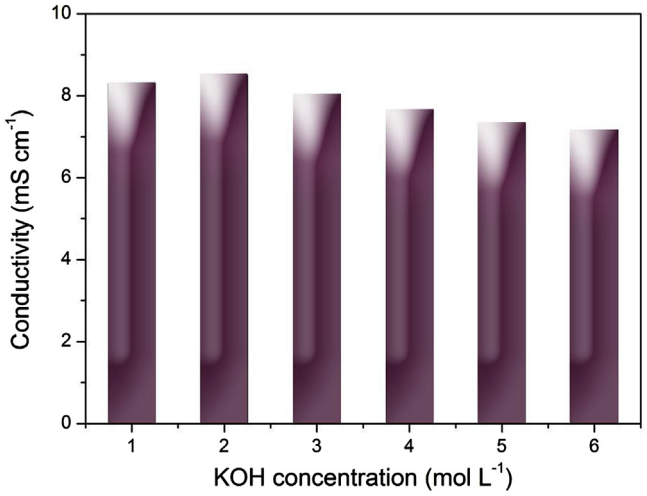

Fig. 7. The alkaline stability of the PGP-NOH membrane in different concentration of KOH solution at 60 °C for 120 h.

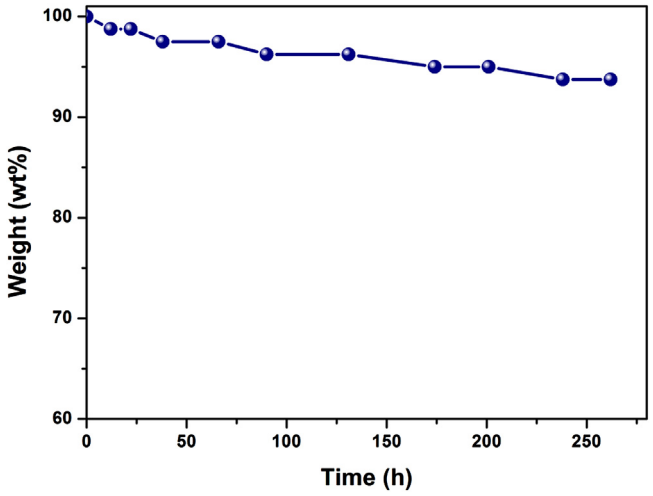

Fig. 8. The oxidative stability of the PGP-NOH membrane in 3 wt% H_2O_2 solution at 60 °C.

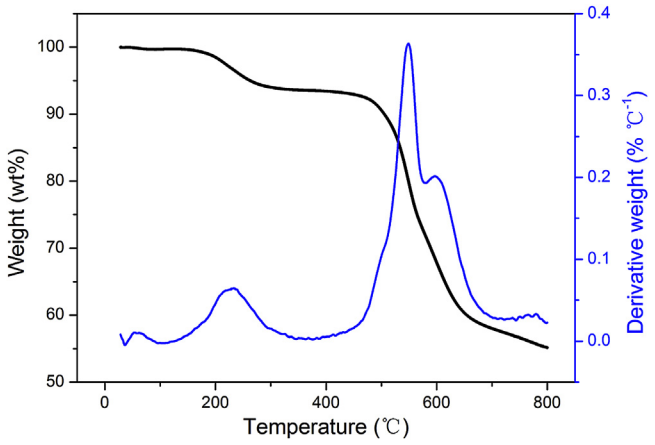

Fig. 9. TGA and DrTGA of PGP-NOH membrane.

Acknowledgments

This research is financially supported by the National Nature Science Foundation of China (No. 1125202; No. 21203204; No. 11175214) and National Nature Science Foundation of Anhui province (No. 1308085QA09).

References

[1] M. Ünlü, J. Zhou, P.A. Kohl, J. Phys. Chem. C 113 (2009) 11416–11423.
[2] R. Bashyam, P. Zelenay, Nature 443 (2006) 63–66.
[3] R. Borup, J. Meyers, B. Pivovar, Y.S. Kim, R. Mukundan, N. Garland, D. Myers, M. Wilson, F. Garzon, D. Wood, P. Zelenay, K. More, K. Stroh, T. Zawodzinski, J. Boncella, J.E. McGrath, M. Inaba, K. Miyatake, M. Hori, K. Ota, Z. Ogumi, S. Miyata, A. Nishikata, Z. Siroma, Y. Uchimoto, K. Yasuda, K.C. Kimjima, N. Iwashita, Chem. Rev. 107 (2007) 3904–3951.
[4] B. Lin, L. Qiu, J. Lu, F. Yan, Chem. Mater. 22 (2010) 6718–6725.
[5] E.H. Yu, X. Wang, U. Krewer, L. Li, K. Scott, Energy Environ. Sci. 5 (2012) 5668–5680.
[6] S. Lu, J. Pan, A. Huang, L. Zhuang, J. Lu, Proc. Natl. Acad. Sci. U. S. A. 105 (2008) 20611.
[7] J.R. Varcoe, R.C.T. Slade, Fuel Cells 5 (2005) 187–200.
[8] J.R. Varcoe, R.C.T. Slade, G.L. Wright, Y.L. Chen, J. Phys. Chem. B 110 (2006) 21041–21049.
[9] E.H. Yu, K. Scott, J. Power Sources 137 (2004) 248–256.
[10] M.R. Hibbs, M.A. Hickner, T.M. Alam, S.K. McIntyre, C.H. Fujimoto, C.J. Cornelius, Chem. Mater. 20 (2008) 2566.
[11] Y. Xiong, Q.L. Liu, Q.H. Zeng, J. Power Sources 193 (2009) 541–546.
[12] M.S. Lee, T. Kim, S.H. Park, C.S. Kim, Y.W. Choi, J. Mater. Chem. 22 (2012) 13928–13931.
[13] M.R. Hibbs, C.H. Fujimoto, C.J. Cornelius, Macromolecules 42 (2009) 8316–8321.
[14] T.N. Danks, R.C.T. Slade, J.R. Varcoe, J. Mater. Chem. 13 (2003) 712–721.
[15] H. Herman, R.C.T. Slade, J.R. Varcoe, J. Membr. Sci. 218 (2003) 147–163.
[16] J.R. Varcoe, Phys. Chem. Chem. Phys. 9 (2007) 1479–1486.
[17] J.R. Varcoe, R.C.T. Slade, E.L.H. Yee, S.D. Poynton, D.J. Driscoll, D.C. Apperley, Chem. Mater. 19 (2007) 2686–2693.
[18] N. Li, Y. Leng, M.A. Hickner, C.Y. Wang, J. Am. Chem. Soc. (2013), http://dx.doi.org/10.1021/ja403671u.
[19] J. Hu, C. Zhang, J. Cong, H. Toyoda, M. Nagatsu, Y. Meng, J. Power Sources 196 (2011) 4483–4490.
[20] C. Zhang, J. Hu, M. Nagatsu, Y. Meng, W. Shen, H. Toyoda, X. Shu, Plasma Process. Polym. 8 (2011) 1024–1032.
[21] C. Zhang, J. Hu, J. Cong, Y. Zhao, W. Shen, H. Toyoda, M. Nagatsu, Y. Meng, J. Power Sources 196 (2011) 5386–5393.
[22] C. Zhang, J. Hu, Y. Meng, M. Nagatsu, H. Toyoda, Chem. Commun. 47 (2011) 10230–10232.
[23] J. Liu, H. Wang, S. Cheng, K.-Y. Chan, J. Membr. Sci. 246 (2005) 95–101.
[24] N. Munichandraiah, K. McGrath, G.K.S. Prakash, R. Aniszfeld, G.A. Olah, J. Power Sources 117 (2003) 98–101.
[25] C. Zhang, J. Hu, M. Nagatsu, X. Shu, H. Toyoda, S. Fang, Y. Meng, Electrochim. Acta 56 (2011) 6033–6040.
[26] C. Qiu, F. Xu, Q.T. Nguyen, Z. Ping, J. Membr. Sci. 255 (2005) 107–115.
[27] J.H. Chen, Q.L. Liu, A.M. Zhu, J. Fang, Q.G. Zhang, J. Membr. Sci. 308 (2008) 171–179.
[28] S. Rajendran, T. Uma, J. Power Sources 88 (2000) 282–285.
[29] B.V. Spitsyn, J.L. Davidson, M.N. Gradoboev, T.B. Galushko, N.V. Serebryakova, T.A. Karpukhina, I.I. Kulakova, N.N. Melnik, Diam. Relat. Mater. 15 (2006) 296–299.
[30] J. Hu, Y. Meng, C. Zhang, S. Fang, Thin Solid Films 519 (2011) 2155–2162.
[31] W.R. Fawcett, G. Liu, A.A. Kloss, J. Chem. Soc. Faraday Trans. 90 (1994) 2697–2701.
[32] E. Loubaki, M. Ourevitch, S. Sicsic, Eur. Polym. J. 27 (1991) 311–317.
[33] N. Sundaraganesan, H. Saleem, S. Mohan, M. Ramalingam, V. Sethuraman, Spectrochim. Acta A 62 (2005) 740–751.
[34] S.B. Roscoe, S. Yitzchaik, A.K. Kakkar, T.J. Marks, Z.Y. Xu, T.G. Zhang, W.P. Lin, G.K. Wong, Langmuir 12 (1996) 5338–5349.
[35] E. Papirer, R. Lacroix, J.-B. Donnet, G. Nanse, P. Fioux, Carbon 33 (1995) 63–72.
[36] D. Briggs, G. Beamson, Anal. Chem. 64 (1992) 1729–1736.
[37] T.I.T. Okpalugo, P. Papakonstantinou, H. Murphy, J. McLaughlin, N.M.D. Brown, Carbon 43 (2005) 153–161.
[38] F.J. Xu, E.T. Kang, K.G. Neoh, Macromolecules 38 (2005) 1573–1580.
[39] K.L. Tan, B.T.G. Tan, E.T. Kang, K.G. Neoh, J. Mater. Sci. 27 (1992) 4056–4060.
[40] A. Welle, J.D. Liao, K. Kaiser, M. Grunze, U. Mäder, N. Blank, Appl. Surf. Sci. 119 (1997) 185–198.
[41] Z. Shi, K.G. Neoh, E.T. Kang, Biomaterials 26 (2005) 501–508.
[42] B.P. Tripathi, M. Kumar, V.K. Shahi, J. Membr. Sci. 360 (2010) 90–101.
[43] H. Long, K. Kim, B.S. Pivovar, J. Phys. Chem. C 116 (2012) 9419–9426.
[44] Y. Wu, C. Wu, T. Xu, F. Yu, Y. Fu, J. Membr. Sci. 321 (2008) 299–308.
[45] H. Biederman, Plasma Polymer Films, Imperial College Press, Covent Gardent, London, 2004.
[46] Z. Jiang, X. Zheng, H. Wu, F. Pan, J. Power Sources 185 (2008) 85–94.